Article

Double Helical Oligoresorcinols Specifically Recognize Oligosaccharides via Heteroduplex Formation through Noncovalent Interactions in Water

Hidetoshi Goto, Yoshio Furusho, and Eiji Yashima

J. Am. Chem. Soc., **2007**, 129 (29), 9168-9174• DOI: 10.1021/ja0730359 • Publication Date (Web): 30 June 2007

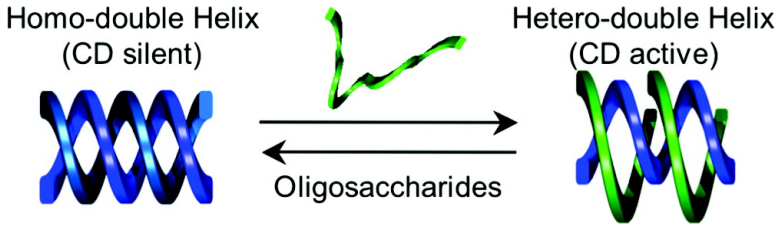

More About This Article

Additional resources and features associated with this article are available within the HTML version:

- Supporting Information
- Links to the 11 articles that cite this article, as of the time of this article download
- Access to high resolution figures
- Links to articles and content related to this article
- Copyright permission to reproduce figures and/or text from this article

View the Full Text HTML

J|A|C|S
ARTICLES
Published on Web 06/30/2007

Double Helical Oligoresorcinols Specifically Recognize Oligosaccharides via Heteroduplex Formation through Noncovalent Interactions in Water

Hidetoshi Goto,[†] Yoshio Furusho,*[,†] and Eiji Yashima*[,†,‡]

Contribution from the Yashima Super-structured Helix Project, Exploratory Research for Advanced Technology (ERATO), Japan Science and Technology Agency (JST), Creation Core Nagoya 101, 2266-22 Anagahora, Shimoshidami, Moriyama-ku, Nagoya 463-0003, Japan, and Institute for Advanced Research, Nagoya University, Chikusa-ku, Nagoya 464-8603, Japan

Received April 30, 2007; E-mail: furusho@yp-jst.jp; yashima@apchem.nagoya-u.ac.jp

Abstract: We report on the oligosaccharide recognition through noncovalent interactions in water based on a unique supramolecular homoduplex-to-heteroduplex transformation of the oligoresorcinol nonamer as a fully artificial receptor. The oligoresorcinol forms a double helix in water, which unravels and entwines upon complexation with specific oligosaccharides with a particular chain length and glucosidic linkage pattern, thus generating the heteroduplex with an excess one-handed helical conformation that can be readily monitored and further quantified by absorption, circular dichroism, and NMR spectroscopies.

Introduction

The development of artificial receptors for saccharides is an intriguing subject of intensive current research.[1] Advances in this field are promising not only for providing insight into the biological functions of saccharides, but also for promoting the development of chemotherapy, because saccharides play essential roles in various cellular activities such as intercellular recognitions.[2] In nature, a sophisticated and exquisite recognition of saccharides is performed by glycoproteins such as lectins, a kind of protein bearing a binding site that participates in the carbohydrate binding through nonpolar as well as hydrogen-bonding interactions.[3] In contrast, the achievement of artificial receptors, which are both effective and genuinely biomimetic, is still a great challenge. There have been reported so far a number of artificial receptors, most of which perform the precise recognition of saccharides in organic media where a hydrogen-bonding interaction acts as the main driving force for the binding.[4−9] However, it remains quite difficult to accomplish saccharide recognition in water by artificial receptors because water molecules can effectively compete for the hydrogen bonds. A notable exception is the receptor system relying on covalent sugar−boronate formation, which is truly effective in water.[1c,10] A limited number of water-soluble receptors with rigid cyclic[11,12] and acyclic[13,14] frameworks and metal complexes[15] can also recognize saccharides in water[12,14,15] or aqueous media.[11,13] Some polysaccharides such as amylose[16] and schizophyllan[17] are known to bind organic compounds in water, although they

[†] ERATO.
[‡] Nagoya University.

(1) For reviews on artificial receptors for saccharides, see: (a) *Host−Guest Chemistry-Mimetic Approaches to Study Carbohydrate Recognition*; Penadés, S. Ed.; Topics in Current Chemistry 218; Springer-Verlag: Berlin, Germany, 2002. (b) Rebek, J., Jr. *Angew. Chem., Int. Ed. Engl.* **1990**, *29*, 245−255. (c) James, T. D.; Sandanayake, K. R. A. S.; Shinkai, S. *Angew. Chem., Int. Ed. Engl.* **1996**, *35*, 1910−1922. (d) Davis, A. P.; Wareham, R. S. *Angew. Chem., Int. Ed.* **1999**, *38*, 2978−2996. (e) Striegler, S. *Curr. Org. Chem.* **2003**, *7*, 81−102. (f) Oshovsky, G. V.; Reinhoudt, D. N.; Verboom, W. *Angew. Chem., Int. Ed.* **2007**, *46*, 2366−2393.

(2) Murray, R. K.; Granner, D. K.; Mayes, P. A.; Rodwell, V. W. *Harper's Illustrated Biochemistry*, 26th ed.; Lange Medical Books: New York, 2003.

(3) For reviews on glycoproteins, see: (a) Lemieux, R. U. *Acc. Chem. Res.* **1996**, *29*, 373−380. (b) Lis, H.; Sharon, N. *Chem. Rev.* **1998**, *98*, 637−674. (c) Beztozzi, C. R.; Kiesling, L. L. *Science* **2001**, *291*, 2357−2364. (d) Dam, T. K.; Brewer, C. F. *Chem. Rev.* **2002**, *102*, 387−429. (e) Jimenez-Barbero, J.; Canada, F. J.; Cuevas, G.; Asensio, J. L.; Aboitiz, N.; Canales, A.; Chavez, M. I.; Fernandez-Alonso, M. C.; Garcia-Herrero, A.; Mari, S.; Vidal, P. *ACS Symp. Ser.* **2006**, *930*, 60−80.

(4) For examples of "face-to-face" recognition by calixarenes and porphyrins in organic media, see: (a) Aoyama, Y.; Tanaka, Y.; Toi, H.; Ogoshi, H. *J. Am. Chem. Soc.* **1988**, *110*, 634−635. (b) Kikuchi, Y.; Kato, Y.; Tanaka, Y.; Toi, H.; Aoyama, Y. *J. Am. Chem. Soc.* **1991**, *113*, 1349−1354. (c) Bonar-Law, R. P.; Sanders, J. K. M. *J. Am. Chem. Soc.* **1995**, *117*, 259−271. (d) Mizutani, T.; Kurahashi, T.; Murakami, T.; Matsumi, N.; Ogoshi, H. *J. Am. Chem. Soc.* **1997**, *119*, 8991−9001. (e) Král, V.; Rusin, O.; Charvátová, J.; Anzenbacher, P., Jr.; Fogl, J. *Tetrahedron Lett.* **2000**, *41*, 10147−10151. (f) Kim, Y.-H.; Hong, J.-I. *Angew. Chem., Int. Ed.* **2002**, *41*, 2947−2950. (g) Landomenou, K.; Bonar-Law, R. P. *Chem. Commun.* **2002**, 2108−2109.

(5) For examples of encapsulation by cyclophane receptors in organic media, see: (a) Bonar-Law, R. P.; Davis, A. P.; Murray, B. A. *Angew. Chem., Int. Ed. Engl.* **1990**, *29*, 1407−1408. (b) Bhattarai, K. M.; Bonar-Law, R. P.; Davis, A. P.; Murray, B. A. *J. Chem. Soc., Chem. Commun.* **1992**, 752−754. (c) Liu, R.; Still, C. *Tetrahedron Lett.* **1993**, *34*, 2573−2576. (d) Anderson, S.; Neidlein, U.; Gramlich, V.; Diederich, F. *Angew. Chem., Int. Ed. Engl.* **1995**, *34*, 1596−1600. (e) Inouye, M.; Miyake, T.; Furusyo, M.; Nakazumi, H. *J. Am. Chem. Soc.* **1995**, *117*, 12416−12425. (f) Davis, A. P.; Wareham, R. S. *Angew. Chem., Int. Ed.* **1998**, *37*, 2270−2273. (g) Bitta, J.; Kubik, S. *Org. Lett.* **2001**, *3*, 2637−2640. (h) Ryan, T. J.; Lecollinet, G.; Velasco, T.; Davis, A. P. *Proc. Natl. Acad. Sci. U.S.A.* **2002**, *99*, 4863−4866. (i) Lecollinet, G.; Dominey, A. P.; Velasco, T.; Davis, A. P. *Angew. Chem., Int. Ed.* **2002**, *41*, 4093−4096. (j) Welti, R.; Diederich, F. *Helv. Chim. Acta* **2003**, *86*, 494−503. (k) Francesconi, O.; Ienco, A.; Moneti, G.; Natovi, C.; Roelens, S. *Angew. Chem., Int. Ed.* **2006**, *45*, 6693−6696.

(6) For examples of cleft receptors in organic media, see: (a) Huang, C.-Y.; Cabell, L. A.; Lynch, V.; Anslyn, E. V. *J. Am. Chem. Soc.* **1992**, *114*, 1900−1901. (b) Huang, C.-Y.; Cabell, L. A.; Lynch, V.; Anslyn, E. V. *J. Am. Chem. Soc.* **1994**, *116*, 2778−2792. (c) Das, G.; Hamilton, A. D. *J. Am. Chem. Soc.* **1994**, *116*, 11139−11140. (d) Cuntze, J.; Owens, L.; Alcázar, V.; Seiler, P.; Diederich, F. *Helv. Chim. Acta* **1995**, *78*, 367−390. (e) Smith, D. K.; Diederich, F. *Chem. Commun.* **1998**, 2501−2502. (f) Benito, J. M.; Gómez-García, M.; Jiménez Blanco, J. L.; Ortiz Mellet, C.; García Fernández, J. M. *J. Org. Chem.* **2001**, *66*, 1366−1372. (g) Tamaru, S.; Yamamoto, M.; Shinkai, S.; Khasanov, A. B.; Bell, T. W. *Chem. Eur. J.* **2001**, *7*, 5270−5276. (h) Tamaru, S.; Shinkai, S.; Khasanov, A. B.; Bell, T. W. *Proc. Natl. Acad. Sci. U.S.A.* **2002**, *99*, 4972−4976.

10.1021/ja0730359 CCC: $37.00

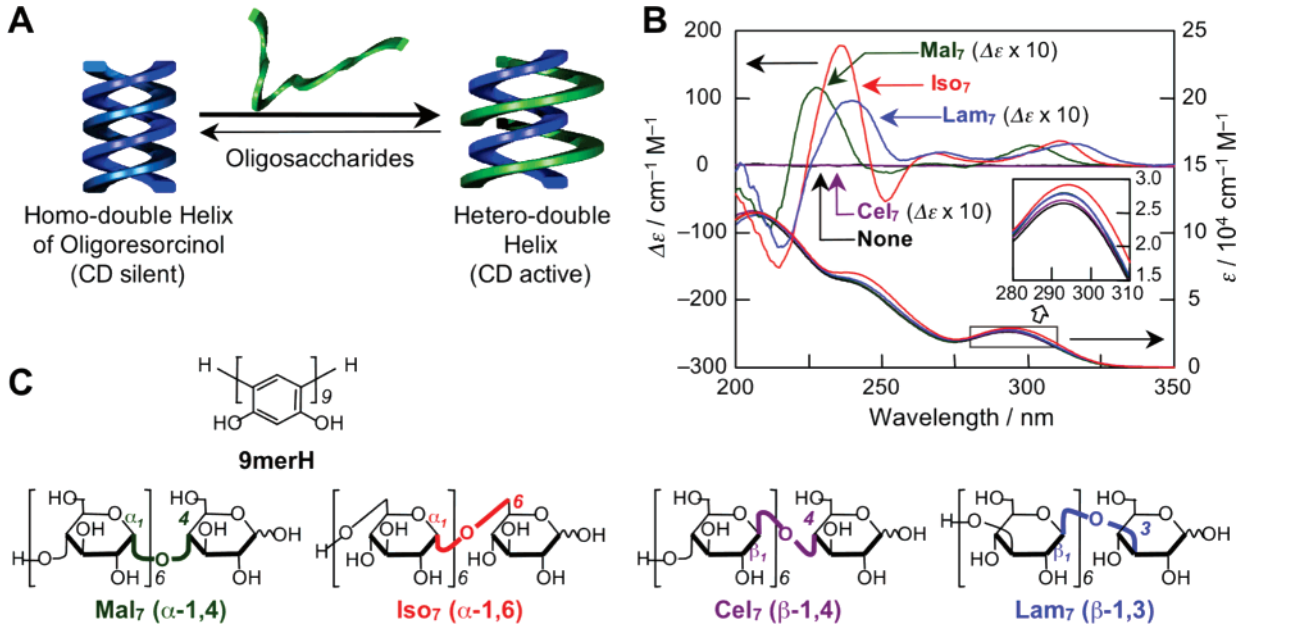

Figure 1. (A) Schematic illustration of the heteroduplex formation of **9merH** with saccharides. (B) CD (0 °C) and absorption (25 °C) spectra of **9merH** in the presence of various oligosaccharide heptamers (**Mal$_7$**, **Iso$_7$**, **Cel$_7$**, and **Lam$_7$**) in H_2O (pH = 4.5−5.5); [**9merH**] = 0.2 mM, [D-glucose unit of oligosaccharides] = 90 mM (**Mal$_7$**, **Iso$_7$**, and **Lam$_7$**) and 3.6 mM (**Cel$_7$**), cell length = 1 mm. The CD intensities of **9merH** with **Mal$_7$**, **Lam$_7$**, and **Cel$_7$** are magnified 10 times. Inset shows expanded absorption spectra in the 280−310 nm region. (C) Structures of **9merH** and oligosaccharide heptamers.

act as hosts rather than guests. However, most of the synthetic receptors have been designed to recognize small saccharides such as mono- and disaccharides, and therefore, the specific recognition of oligosaccharides in water is still considered underdeveloped[1,10d,10f,10g,13a,15a,15d] and requires a new conceptual approach.

We now report a unique and conceptually new oligosaccharide recognition in water using a double helical oligoresorcinol as a specific receptor which unravels and entwines upon complexation with oligosaccharides with a particular chain length and glucosidic linkage pattern, thus generating an induced circular dichroism (CD) due to the heteroduplex formation with an excess one-handed helical conformation (Figure 1A).

Results and Discussion

Oligosaccharides Recognition in Water. Recently, we reported the first example of fully artificial double helices that are formed in water by the self-assembly of oligoresorcinols, a kind of oligophenol, as a result of interstrand aromatic interactions in water.[18] The oligoresorcinol nonamer (**9merH**) (Figure 1C) is long enough to form a double helix as the major species in water, but it dissociates into individual strands in the presence of an increasing volume of organic solvents such as methanol at more than 28 vol %, indicating that the double helix formation

(7) For examples of tripodal receptors in organic media, see: (a) Mazik, M.; Bandmann, H.; Sicking, W. *Angew. Chem., Int. Ed.* **2000**, *39*, 551−554. (b) Mazik, M.; Sicking, W. *Chem. Eur. J.* **2001**, *7*, 664−670. (c) Kim, H.-J.; Kim, Y.-H.; Hong, J.-I. *Tetrahedron Lett.* **2001**, *42*, 5049−5052. (d) Vacca, A.; Nativi, C.; Cacciarrini, M.; Pergoli, R.; Roelens, S. *J. Am. Chem. Soc.* **2004**, *126*, 16456−16465. (e) Abe, H.; Aoyagi, Y.; Inouye, M. *Org. Lett.* **2005**, *7*, 59−61. (f) Nativi, C.; Cacciarini, M.; Francesconi, O.; Vacca, A.; Moneti, G.; Ienco, A.; Roelens, S. *J. Am. Chem. Soc.* **2007**, *129*, 4377−4385.

(8) For examples of foldamer receptors in organic media, see: (a) Inouye, M.; Waki, M.; Abe, H. *J. Am. Chem. Soc.* **2004**, *126*, 2022−2027. (b) Hou, J.-L.; Shao, X.-B.; Chen, G.-J.; Zhou, Y.-X.; Jiang, X.-K.; Li, Z.-T. *J. Am. Chem. Soc.* **2004**, *126*, 12386−12394.

(9) For self-assembled receptors in organic media, see: Ishi-i, T.; Mateos-Timoneda, M. A.; Timmerman, P.; Crego-Calama, M.; Reinhoudt, D. N.; Shinkai, S. *Angew. Chem., Int. Ed.* **2003**, *42*, 2300−2305.

(10) For examples of boronate-based receptors, see: (a) Tsukagoshi, K.; Shinkai, S. *J. Org. Chem.* **1991**, *56*, 4089−4091. (b) Nagai, Y.; Kobayashi, K.; Toi, H.; Aoyama, Y. *Bull. Chem. Soc. Jpn.* **1993**, *66*, 2965−2971. (c) James, T. D.; Sandanayake, K. R. A. S.; Shinkai, S. *Nature* **1995**, *374*, 345−347. (d) Ikeda, M.; Shinkai, S.; Osuka, A. *Chem. Commun.* **2000**, 1047−1048. (e) Lewis, P. T.; Davis, C. J.; Cabell, L. A.; He, M.; Read, M. W.; McCarroll, M. E.; Strongin, R. M. *Org. Lett.* **2000**, *2*, 589−592. (f) Sugasaki, A.; Sugiyasu, K.; Ikeda, M.; Takeuchi, M.; Shinkai, S. *J. Am. Chem. Soc.* **2001**, *123*, 10239−10244. (g) Zhong, Z.; Anslyn, E. V. *J. Am. Chem. Soc.* **2002**, *124*, 9014−9015. (h) Jiang, S.; Escobedo, J. O.; Kim, K. K.; Alptürk, O.; Samoei, G. K.; Fakayode, S. O.; Warner, I. M.; Rusin, O.; Strongin, R. M. *J. Am. Chem. Soc.* **2006**, *128*, 12221−12228. (i) Trupp, S.; Schweitzer, A.; Mohr, G. J. *Org. Biomol. Chem.* **2006**, *4*, 2965−2968.

(11) For examples of macrocyclic receptors in aqueous media containing organic solvents, see: (a) Král, V.; Rusin, O.; Schmidtchen, F. P. *Org. Lett.* **2001**, *3*, 873−876. (b) Rusin, O.; Lang, K.; Král, V. *Chem. Eur. J.* **2002**, *8*, 655−662.

(12) For examples of macrocyclic receptors in water, see: (a) Kobayashi, K.; Asakawa, Y.; Kato, Y.; Aoyama, Y. *J. Am. Chem. Soc.* **1992**, *114*, 10307−10313. (b) Coterón, J. M.; Vicent, C.; Bosso, C.; Penadés, S. *J. Am. Chem. Soc.* **1993**, *115*, 10066−10076. (c) Jiménez-Barbero, J.; Junquera, E.; Martín-Pastor, M.; Sharma, S.; Vicent, C.; Penadés, S. *J. Am. Chem. Soc.* **1995**, *117*, 11198−11204. (d) Morales, J. C.; Penadés, S. *Angew. Chem., Int. Ed.* **1998**, *37*, 654−657. (e) Rusin, O.; Král, V. *Chem. Commun.* **1999**, 2367−2368. (f) Klein, E.; Crump, M. P.; Davis, A. P. *Angew. Chem., Int. Ed.* **2005**, *44*, 298−302.

(13) For examples of acyclic receptors in aqueous media containing organic solvents, see: (a) Dukh, M.; Saman, D.; Lang, K.; Pouzar, V.; Cerny, I.; Drasar, P.; Král, V. *Org. Biomol. Chem.* **2003**, *1*, 3458−3463. (b) Schmuck, C.; Schwegmann, M. *Org. Lett.* **2005**, *7*, 3517−3520. (c) Waki, M.; Abe, H.; Inouye, M. *Chem. Eur. J.* **2006**, *12*, 7839−7847.

(14) For examples of acyclic receptors in water, see: (a) Sugimoto, N.; Miyoshi, D.; Zou, J. *Chem. Commun.* **2000**, 2295−2296. (b) Mazik, M.; Cavga, H. *J. Org. Chem.* **2006**, *71*, 2957−2963.

(15) For examples of metal complex-based receptors in water, see: (a) He, M.; Johnson, R. J.; Escobedo, J. O.; Beck, P. A.; Kim, K. K.; St. Luce, N. N.; Davis, C. J.; Lewis, P. T.; Fronczek, F. R.; Melancon, B. J.; Mrse, A. A.; Treleaven, W. D.; Strongin, R. M. *J. Am. Chem. Soc.* **2002**, *124*, 5000−5009. (b) Striegler, S.; Dittel, M. *J. Am. Chem. Soc.* **2003**, *125*, 11518−11524. (c) Strieger, S.; Dittel, M. *Inorg. Chem.* **2005**, *44*, 2728−2733. (d) Alptürk, O.; Rusin, O.; Fakayode, S. O.; Wang, W.; Escobedo, J. O.; Warner, I. M.; Crowe, W. E.; Kral, V.; Pruet, J. M.; Strongin, R. M. *Proc. Natl. Acad. Sci. U.S.A.* **2006**, *103*, 9756−9760.

(16) For examples of amylose as host, see: (a) Star, A. F.; Steuerman, D. W.; Heath, J. R.; Stoddart, J. F. *Angew. Chem., Int. Ed.* **2002**, *41*, 2508−2512. (b) Star, A.; Stoddart, J. F. *Macromolecules* **2002**, *35*, 7516−7520.

(17) For examples of schizophyllan as host, see: (a) Numata, M.; Asai, M.; Kaneko, K.; Bae, A.-H.; Hasegawa, T.; Sakurai, K.; Shinkai, S. *J. Am. Chem. Soc.* **2005**, *127*, 5875−5884. (b) Numata, M.; Tamesue, S.; Fujisawa, T.; Haraguchi, S.; Hasegawa, T.; Bae, A.-H.; Li, C.; Sakurai, K.; Shinkai, S. *Org. Lett.* **2006**, *8*, 5533−5536.

(18) (a) Goto, H.; Katagiri, H.; Furusho, Y.; Yashima, E. *J. Am. Chem. Soc.* **2006**, *128*, 7176−7178. (b) Goto, H.; Furusho, Y.; Yashima, E. *J. Am. Chem. Soc.* **2007**, *129*, 109−112. (c) Furusho, Y.; Yashima, E. *Chem. Rec.* **2007**, *7*, 1−11.

is sensitive to its environment.[18a] This unique dynamic property was anticipated to construct more complex supramolecular assemblies with specific guest molecules such as saccharides in water. In fact, we have recently found that the double helix of **9merH** was unwound by β- and γ-cyclodextrins (CyDs), naturally occurring α-1,4-linked cyclic oligomers of D-glucose with a chiral hydrophobic cavity (heptamer and octamer, respectively), thus forming a twisted [3]pseudorotaxane with a controlled helicity in water, resulting from the encapsulation of the single **9merH** strands into the CyD cavities.[18b] This unique pseudorotaxane formation is accompanied by the appearance of an induced CD in the absorption region of the **9merH** backbone, whereas it hardly occurred with α-CyD (cyclic hexamer). These promising results promoted us to investigate if the **9merH** could be used as a versatile receptor for the specific recognition of linear oligosaccharides with a different chain length and glucosidic linkage in water.

We first investigated the binding affinities of **9merH** toward a series of linear oligosaccharide heptamers consisting of D-glucose units with a different glucosidic linkage, α-1,4-D-maltoheptaose (**Mal$_7$**), α-1,6-D-isomaltoheptaose (**Iso$_7$**), β-1,4-D-celloheptaose (**Cel$_7$**), and β-1,3-D-laminariheptaose (**Lam$_7$**) (Figure 1C), and the results were compared with that of the cyclic maltoheptaose, β-CyD.

Figure 1B shows the CD and absorption spectra of **9merH** in the presence of the heptamers in water. **9merH** exists as an equimolar mixture of the right- and left-handed double helices so that it is CD silent. However, distinct CDs were induced in the presence of **Mal$_7$**, **Iso$_7$**, and **Lam$_7$** in the absorption region of the **9merH** (200−350 nm) and accompanied by a weak, but measurable, increase in the absorption intensities (hyperchromic effect), suggesting that the double helix of **9merH** is unwound by the oligosaccharide strands, thus forming a heteroduplex with an excess one-handed helical conformation (Figure 1A) as observed in the twisted rotaxane formation with CyDs.[18b] The observed CD spectral patterns and intensities and the hyperchromic effect were significantly dependent on the oligosaccharide structures; the **9merH** showed a remarkable selectivity for α-1,6-D-**Iso$_7$** among the oligosaccharides with a different glucosidic linkage that forms the heteroduplex and exhibited the most intense induced CD in water, whereas **Mal$_7$** and **Lam$_7$** gave a weak CD with different Cotton effect patterns from that of **Iso$_7$** and caused hyperchromic effects, but to a lesser extent. These results indicate that the resultant heteroduplexes may take a similar but slightly different helical conformation via an induced-fit mechanism regulated by the unique oligosaccharide structures.

The CD spectral pattern of **9merH** induced by the linear maltoheptaose **Mal$_7$** was quite similar to that induced by the cyclic analogue β-CyD (Supporting Information Figure S1),[19] suggesting that the **9merH** may have a similar helical conformation upon complexation with the linear and cyclic maltoheptaoses. Because of solubility limit of **Cel$_7$** in water, a relatively small amount of **Cel$_7$** could be used, giving no CD in the **9merH** chromophore region.

To gain a further insight into the *racemic* homoduplex-to-*preferred-helical*-heteroduplex transformation process, the UV and CD titration experiments of **9merH** with **Mal$_7$**, **Iso$_7$**, and **Lam$_7$** were performed and their association constants (K_a) were attempted to estimate (Figure 2, Supporting Information Figures S2 and S3).[19] The CD intensities increased with the increasing concentration of **Mal$_7$**, **Iso$_7$**, and **Lam$_7$** accompanied with a synchronous increase in their absorption intensities. Particularly, the changes in the CD and absorption spectra for **Iso$_7$** were significant due to its strong binding to **9merH**. The stoichiometries of the heteroduplex formations were then evaluated by the continuous variation plot (Job plot), but because of weak interactions between **9merH** and **Mal$_7$** and **Lam$_7$**, a clear 1:2 stoichiometry was obtained only for the **9merH**−**Iso$_7$** system (Figure 2). The titration data using **Iso$_7$** were analyzed based on the 1:2 stoichiometry according to eqs 1 and 2, giving the K_a value of $(2.5 \pm 1.7) \times 10^3$ M^{-3} estimated by the UV titrations at 0 °C; this value is in good agreement with that estimated by the CD titrations at 0 °C ($(2.7 \pm 1.6) \times 10^3$ M^{-3}) and is smaller than that for the **9merH**−β-CyD system ($(1.3 \pm 0.7) \times 10^7$ M^{-3}).[18b] In the same way, the K_a values for **Mal$_7$** and **Lam$_7$** were estimated to be $(3.9 \pm 1.5) \times 10^2$ M^{-3} and 8.1 ± 3.4 M^{-3} based on the CD titrations, respectively, by assuming the 1:2 stoichiometry (Supporting Information Figures S2 and S3).[19] Thus, the binding affinities of the oligosaccharides to **9merH** decrease in the following order: β-CyD > **Iso$_7$** > **Mal$_7$** > **Lam$_7$**.

An indication of such a heteroduplex formation could be detected by ^{1}H NMR (see below for a more detailed discussion). In addition, heating a solution mixture of **9merH** and **Iso$_7$** ([**9merH**] = 0.2 mM, [**Iso$_7$**] = 5.4 mM) caused a gradual decrease in the Cotton effects, which further completely disappeared at around 70 °C, but markedly increased upon cooling in the range from 0 to −10 °C (Supporting Information Figure S4).[19] These results clearly indicated the dynamic nature in the homoduplex-to-heteroduplex transformation process depending on the concentration of the oligosaccharides and temperature.

Chain-Length Dependence of the Binding Affinity. The binding affinity of **9merH** toward the oligosaccharide heptamers was found to be sensitive to the glucosidic linkages, and **9merH** showed a high selectivity toward **Iso$_7$** with the α-1,6-linkage. To understand the nature of the heteroduplex formation in more detail, the chain-length dependence of the binding affinity of **9merH** was explored using a series of oligoisomaltoses (from D-glucose (**Glu**) to **Iso$_7$**) and its polymer (dextran (**Dex**)) by means of UV and CD spectroscopies (Figure 3, parts A and B). In each measurement, the concentrations of the saccharides were kept constant at 90 mM glucose units in order to allow the direct comparison of the affinities of **9merH** to the saccharides. **Glu** and **Iso$_2$**−**Iso$_5$** induced no CD at all in the **9merH** chromophore region, whereas a longer **Iso$_6$** exhibited a weak, but detectable CD; the CD intensity further increased with the increasing chain length of the isomaltooligosaccharides and reached the maximum value at the average repeating glucose unit (n) = 20 (**Dex$_{20}$**, molecular weight distribution (MWD) = 1.60) along with a stronger hyperchromicity. The induced CD patterns were virtually the same, irrespective of the chain lengths, as shown in Figure 3A. This indicates that the heteroduplex formation becomes more favorable with longer isomaltooligosaccharides and that essentially the same helical conformations with an excess one-handedness were induced in the **9merH** by the longer oligosaccharides, but their excess of the one helical sense increased to the oligosaccharides with a

(19) See the Supporting Information.

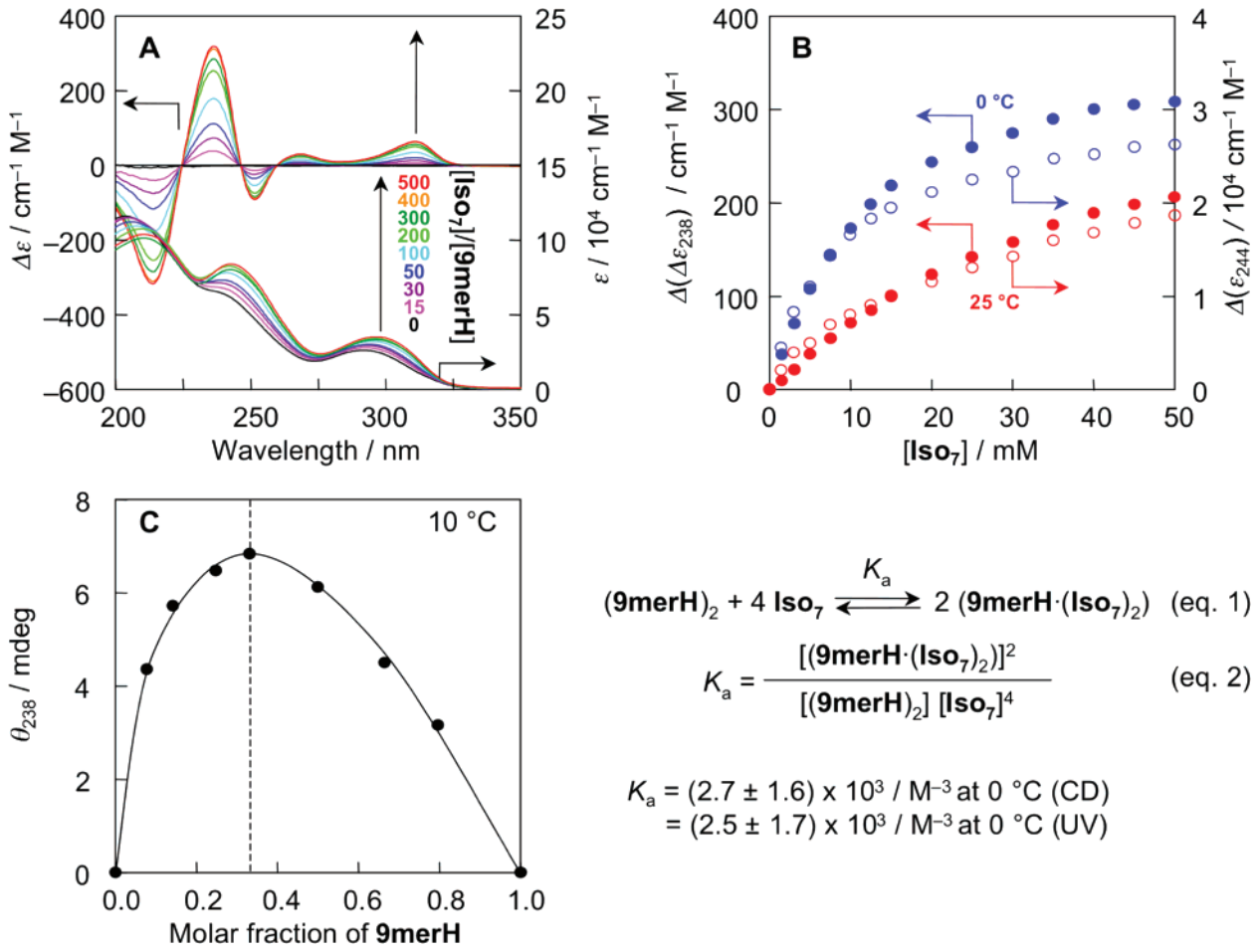

Figure 2. (A) CD and absorption spectra of **9merH** with $\mathbf{Iso_7}$ in H_2O (pH = 5.0−5.2) at 0 °C; [**9merH**] = 0.1 mM, [$\mathbf{Iso_7}$] = 0−50 mM, cell length = 2 mm. (B) Changes of molar CD at 238 nm $\Delta(\Delta\epsilon_{238})$ (filled circles) and molar absorptivity at 244 nm $\Delta(\epsilon_{244})$ (open circles) of **9merH** with $\mathbf{Iso_7}$ at 0 (blue) and 25 °C (red). (C) Job's plot of θ_{238} of **9merH** with $\mathbf{Iso_7}$ in H_2O (pH = 5.0−5.2) at 10 °C. The total concentration is 4 mM, and the CD intensities of the complex are plotted vs the molar fraction of **9merH**; cell length = 0.1 mm.

particular chain length in which the **9merH** strand may form a full-match heteroduplex hybrid. A similar chain-length dependence of the binding affinity of **9merH** was observed for maltooligosaccharides ($\mathbf{Mal_2}$−$\mathbf{Mal_7}$) and laminarioligosaccharides ($\mathbf{Lam_2}$−$\mathbf{Lam_7}$) (Figure 3C−F).

As well as the chain lengths of the oligosaccharides, those of the oligoresorcinols are anticipated to influence the effective heteroduplex formation. In fact, very weak CDs with similar Cotton effect patterns were observed when smaller oligoresorcinols (a trimer (**3merH**) and a hexamer (**6merH**)) (18 mM monomer units) were mixed with $\mathbf{Dex_{20}}$ (120 mM glucose units) in water at 25 °C; the molar CD values at around 240 nm ($\Delta\epsilon$/ cm^{-1} M^{-1} $unit^{-1}$) significantly decreased as follows: **9merH** (42), **6merH** (2.3), and **3merH** (0.03) (Supporting Information Figure S5).[19] This is probably because **3merH** and **6merH**, which exist as a single strand, and a ca. 1:1 mixture of the single strand and the double helix, respectively,[18a] are too short to effectively bind the oligosaccharide in water.

Structure of the Heteroduplex of 9merH with Dextran. We next investigated the stoichiometry, structure, and binding behavior of the strongly intertwined **9merH**−$\mathbf{Dex_{20}}$ heteroduplex in detail. The titration experiments of **9merH** with $\mathbf{Dex_{20}}$ were then performed using UV, CD, and ^{1}H NMR spectroscopies under identical conditions (Figure 4). The CD titration showed that the CD intensity increased with the increasing concentration of $\mathbf{Dex_{20}}$ and reached an almost maximum value at 5 equiv of $\mathbf{Dex_{20}}$ accompanied by a synchronous increase in their absorption intensities (Figure 4A). This indicates that 5 equiv of $\mathbf{Dex_{20}}$ are sufficient to quantitatively produce the heteroduplex with **9merH**, resulting in inducing an almost one-handed helical conformation. In sharp contrast, a large amount of $\mathbf{Iso_7}$ (>400 equiv) was required to induce a preferred handed heteroduplex (Figure 2).

In addition, such a heteroduplex formation of **9merH** with $\mathbf{Dex_{20}}$ was directly detected by ^{1}H NMR; the aromatic proton resonances located inside the **9merH** homoduplex (3-H in Figure 4B) were shifted downfield in the presence of $\mathbf{Dex_{20}}$ because the aromatically π-stacked double helix of **9merH** is unwound by the $\mathbf{Dex_{20}}$ strands, thus forming a heteroduplex with a bias in the twist sense. Similar downfield shifts of the 3-H protons were also observed during the pseudorotaxane formation between **9merH** and CyDs.[18b] The homoduplex-to-heteroduplex transformation process is in slow exchange on the NMR time scale, and therefore, the molar fractions of the heteroduplex were estimated to be 39%, 57%, 81%, and 95% in the presence of 0.6, 1, 2, and 5 equiv of $\mathbf{Dex_{20}}$ based on the integral ratio of the downfield 3-H protons and other aromatic protons (Figure 4B); these values are consistent with those estimated on the basis of the maximum CD value for the **9merH**−$\mathbf{Dex_{20}}$ duplex. The CD and UV titration data combined with a job plot (almost

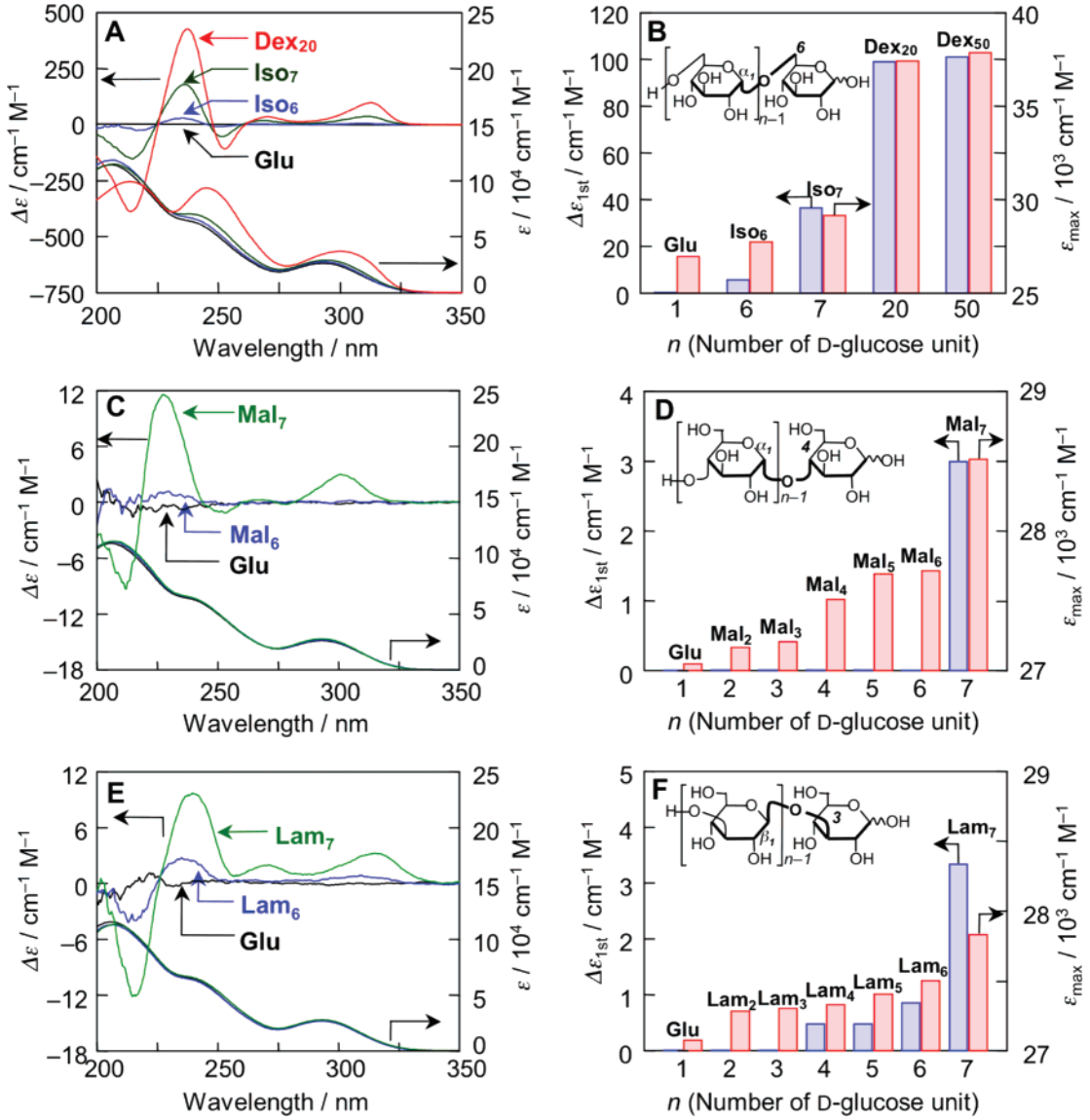

Figure 3. (A, C, and E) CD (0 °C) and absorption (25 °C) spectra of **9merH** with **Glu**, **Iso$_6$**, **Iso$_7$**, and **Dex$_{20}$** (A), **Glu**, **Mal$_6$**, and **Mal$_7$** (C), and **Glu**, **Lam$_6$**, and **Lam$_7$** (E) in H_2O (pH = 4.0−5.5); [**9merH**] = 0.2 mM, [D-glucose unit of saccharides] = 90 mM, cell length = 1 mm. (B, D, and F) Chain-length dependence of molar CD of the first Cotton at ca. 310 nm ($\Delta\epsilon_{first}$, 0 °C) (blue bar) and molar absorptivity at ca. 300 nm (ϵ_{max}, 25 °C) (red bar) of **9merH** with **Glu**, **Iso$_6$**, **Iso$_7$**, **Dex$_{20}$**, and **Dex$_{50}$** (B), **Glu** and **Mal$_2$**−**Mal$_7$** (D), and **Glu** and **Lam$_2$**−**Lam$_7$** (F) in H_2O (pH = 4.0−5.5).

1:1 stoichiometry) roughly provided the association constant (K_a) of **9merH** to **Dex$_{20}$** to be (3.5 ± 1.2) × 10^3 M^{-1} (CD) or (3.6 ± 1.2) × 10^3 M^{-1} (UV) at 25 °C, based on the eqs 3 and 4 (Figure 5).

Furthermore, the induced CD of the **9merH**−**Dex$_{20}$** duplex ([**9merH**] = 0.1 mM, [**Dex$_{20}$**] = 0.5 mM) in water gradually decreased by adding increasing volumes of methanol and almost disappeared in the presence of 40 vol % of methanol as a result of the unwinding of the heteroduplex (Supporting Information Figure S6).[19] In addition, the van't Hoff analysis within the range of 10−50 °C revealed that the main driving force for the heteroduplex formation is a favorable enthalpy term (ΔH = −31.9 ± 0.5 kcal mol^{-1} and ΔS = −91 ± 2 cal mol^{-1} K^{-1}), i.e., sugar/aromatic interactions in water, as in the case of lectin−saccharide complex formation (Supporting Information Figure S7).[3,19]

Further evidence for the **9merH**−**Dex$_{20}$** heteroduplex formation was obtained from the diffusion-ordered ^{1}H NMR spectroscopy (DOSY) experiments (Table 1).[20] The diffusion coefficients (D) of the **9merH** and **Dex$_{20}$** in D_2O were 1.9 × 10^{-10} and 1.1 × 10^{-10} $m^2 \cdot s^{-1}$, respectively. However, upon mixing each solution, the D value of the **9merH** moiety in the assembly was halved and became 1.0 × 10^{-10} $m^2 \cdot s^{-1}$, which is almost the same as that of **Dex$_{20}$** itself. In contrast, the D value of the **Dex$_{20}$** moiety showed almost no change after complexation. These data also support the fact that the unwound single strands of **9merH** formed a 1:1 heteroduplex with **Dex$_{20}$** (Figure 1A).

In order to propose a possible structure for the 1:1 **9merH**−**Dex$_{20}$** heteroduplex, the 2D NOESY spectrum was recorded. Several nuclear Overhauser effect (NOE) cross-peaks were observed between the aromatic protons of **9merH** and the

(20) (a) Cohen, Y.; Avram, L.; Frish, L. *Angew. Chem., Int. Ed.* **2005**, *44*, 520−554. (b) Haino, T.; Matsumoto, Y.; Fukazawa, Y. *J. Am. Chem. Soc.* **2005**, *127*, 8936−8937. (c) Ikeda, M.; Tanaka, Y.; Hasegawa, T.; Furusho, Y.; Yashima, E. *J. Am. Chem. Soc.* **2006**, *128*, 6806−6807. (d) Morris, K. F.; Becker, B. A.; Valle, B. C.; Warner, I. M.; Larive, C. K. *J. Phys. Chem. B* **2006**, *110*, 17359−17369. (e) Ohkawa, H.; Ligthart, G. B. W. L.; Sijbesma, R. P.; Meijer, E. W. *Macromolecules* **2007**, *40*, 1453−1459.

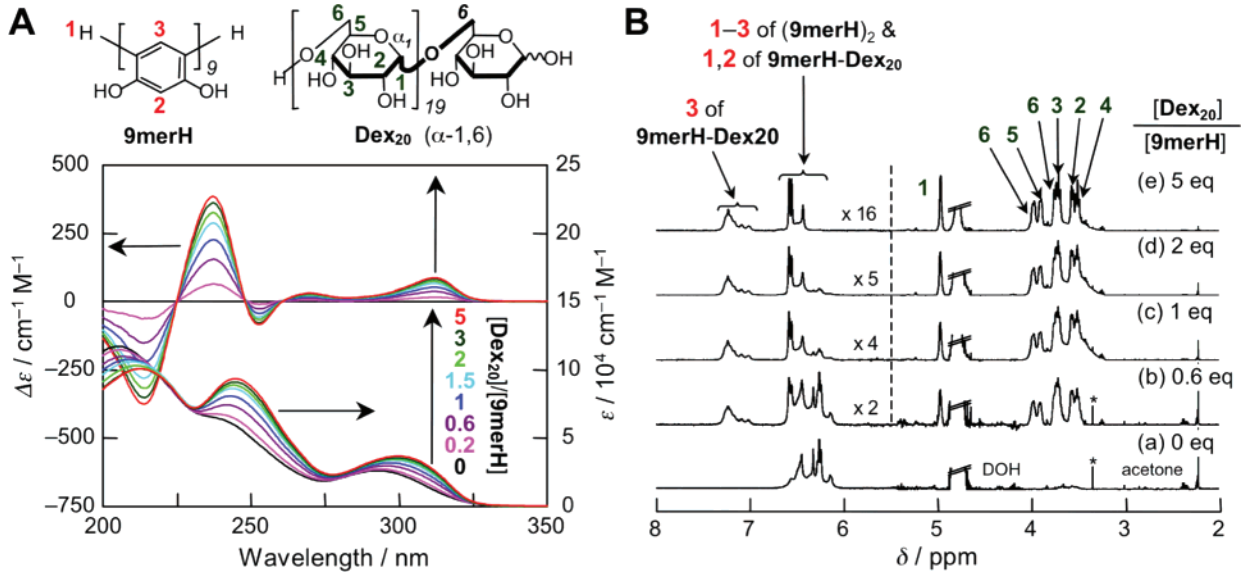

Figure 4. CD and absorption (A) and ^{1}H NMR (B) spectral changes of **9merH** with **Dex$_{20}$** in D_2O (pD = 5.3−6.8) at 25 °C; [**9merH**] = 1 mM, [**Dex$_{20}$**]/[**9merH**] = 0−5.

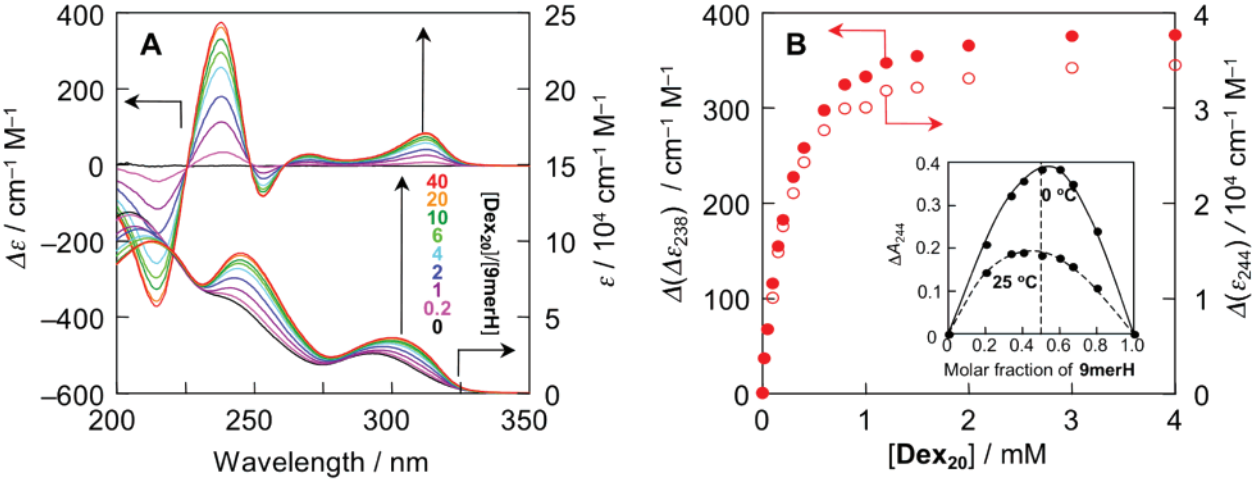

$$(\mathbf{9merH})_2 + 2\ \mathbf{Dex_{20}} \underset{}{\overset{K_a}{\rightleftharpoons}} 2\ (\mathbf{9merH\text{–}Dex_{20}}) \qquad \text{(eq. 3)} \quad K_a = (3.5 \pm 1.2) \times 10^3\ /\ M^{-1}\ \text{(CD)} = (3.6 \pm 1.2) \times 10^3\ /\ M^{-1}\ \text{(UV)}$$

$$K_a = \frac{[(\mathbf{9merH\text{–}Dex_{20}})]^2}{[(\mathbf{9merH})_2]\,[\mathbf{Dex_{20}}]^2} \qquad \text{(eq. 4)}$$

Figure 5. (A) CD and absorption spectra of **9merH** with **Dex$_{20}$** in H_2O (pH = 5.0−5.2) at 25 °C; [**9merH**] = 0.1 mM, [**Dex$_{20}$**] = 0−4 mM, cell length = 2 mm. (B) Changes of molar CD at 238 nm $\Delta(\Delta\epsilon_{238})$ (filled circles) and molar absorptivity at 244 nm $\Delta(\epsilon_{244})$ (open circles) of **9merH** with **Dex$_{20}$** at 25 °C. Inset: Job's plots of θ_{238} of **9merH** with **Dex$_{20}$** in H_2O (pH = 5.0−5.2) at 25 and 0 °C. The total concentration is 0.4 mM, and the absorbances of the complex are plotted vs the molar fraction of **9merH**; cell length = 1 mm.

aliphatic protons of **Dex$_{20}$** in D_2O (Figure 6A, Supporting Information Figures S8 and S9).[19] The 3-H protons on the hydrophobic rim of **9merH** showed clear NOE cross-peaks with all the protons of **Dex$_{20}$**, which include intense NOE cross-peaks with 1-H and 6-H protons of **Dex$_{20}$**, whereas the 2-H protons on the hydrophilic rim of **9merH** exhibited cross-peaks only with the 2-H and 4-H protons located in the hydrophilic face of the glucose units (see Figure 4A for the positions of the protons). On the basis of these NOE results, a possible model for the heterodouble helix of **9merH** with a dextran 20mer was constructed in such a way that the 20mer strand can be entwined with the 5_1-helical strand of **9merH** and subjected to the structure optimization by molecular mechanics calculations

Table 1. Diffusion Coefficients (*D*) of **9merH**, Dextrans (**Dex**s), and Their Complexes[a]

system	concn (mM)	*D* (10^{-10} m^2 s^{-1}) **9merH**	**Dex**	water
9merH	2	1.93		18.6
Dex$_{20}$	6		1.07	19.3
9merH/Dex$_{20}$	2/6	1.01	1.14	18.9
Dex$_{50}$	2.4		0.73	18.9
9merH/Dex$_{50}$	2/2.4	0.73	0.74	18.9

[a] Measured in D_2O at 25 °C.

(Figure 6B). After optimization of the structure of the heteroduplex, we found that the hydrophobic faces of the glucose units

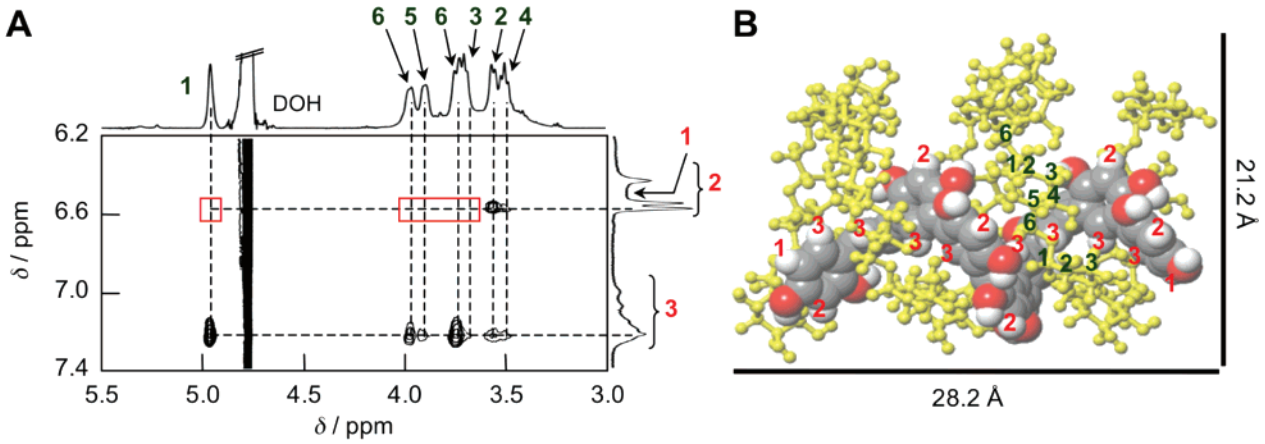

Figure 6. (A) Partial NOESY spectrum of **9merH** with **Dex$_{20}$** in D_2O at 25 °C; mixing time = 0.3 s, [**9merH**] = 2 mM, [**Dex$_{20}$**] = 6 mM. (B) The molecular mechanics calculated structure of the heteroduplex of **9merH** with a dextran 20mer. The predominant helix sense of the heteroduplex is tentative.

contact the hydrophobic groove of the **9merH** strand, resulting in the formation of an intertwined heteroduplex with a controlled helicity, which is in good agreement with the observed NOEs (Supporting Information Table S1).[19] This model also supports the 1:1 complexation of the **9merH** and **Dex$_{20}$** strands, and the helical conformation of **9merH** is similar to that complexed with β-CyD.[18b]

Conclusion

We found that the water-soluble **9merH** has a unique ability as a specific receptor for oligosaccharides via the heterodouble helix formation through noncovalent sugar/aromatic interactions in water. Its binding affinity is highly affected by the chain length and glucosidic linkage patterns of oligosaccharides, and **9merH** exhibits an extremely high selectivity to α-1,6-D-isomaltooligosaccharides. Since the oligoresorcinols have simple structures and are readily accessible by synthesis, we expect that it is possible to design and synthesize tailor-made host molecules based on the oligoresorcinols that can bind and recognize other oligosaccharides physiologically and biologically more important, which is currently in progress.

Experimental Section

Instruments. The solution pH was measured using a DKK-TOA GST-5428S pH meter (Tokyo, Japan). The NMR spectra were obtained using a Varian UNITY INOVA 500AS spectrometer operating at 500 MHz for ^{1}H. The chemical shifts are reported in parts per million (δ) downfield from acetone dissolved in D_2O as the external standard in D_2O. The DOSY experiments were carried out by using pulsed field gradient with the BPPSTE pulse sequence.[20] The absorption and CD spectra were measured by a JASCO V-570 spectrophotometer and a JASCO J-820 spectropolarimeter, respectively. The temperature was controlled by a JASCO PTC-423L apparatus (−10 to 80 °C). The pDs (−log[D^+]) were calculated by the equation, pD = pH reading + 0.40.[21]

Materials. The oligoresorcinol nonamer (**9merH**) was synthesized according to the previous literature.[18a] The saccharides were purchased from suppliers as follows: maltooligosaccharides, Hayashibara Biochemical laboratories Inc., Okayama, Japan; cellooligosaccharides, Institute of Chemistry, Slovak Academy of Sciences, Bratislava, Slovakia; isomaltooligosaccharides and laminarioligosaccharides, Seikagaku Corp., Tokyo, Japan; D-(+)-glucose, Wako Pure Chemical Industries, Ltd., Osaka, Japan; dextrans (**Dex$_{20}$** (molecular weight = 3260, MWD = 1.60, n = 20)) and **Dex$_{50}$** (molecular weight = 8110, MWD = 1.43, n = 50)) for SEC standards, Fluka, Buchs, Switzerland. The distilled water and D_2O (99.9 atom %D) were purchased from Wako and Cambridge Isotope Laboratories (Andover, MA), respectively, and were degassed with argon prior to use.

Molecular Modeling and Calculations. The molecular modeling and molecular mechanics calculations were performed using the Compass Force Field as implemented in the Materials Studio software (version 4.0; Accerlys Software Inc.). The model of the heteroduplex of **9merH** and a dextran 20mer was constructed using Materials Visualizer in the Materials Studio. The parameter, "relative electric" was set to 4 which is the recommended value for the calculations in water.

The calculated model of the double helix of **9merH** was used according to the previous literature.[18a,18b] Charges on the atoms of the oligomers were calculated using the charge equilibration (QEq) in the Materials Studio; the total charges of the molecules were set to zero.

The initial model of a dextran 20mer was constructed as described below. First, the structure of α-D-glucose was optimized using the Smart Minimizer of the Discover module until the root-mean-square value became less than 0.1 kcal mol^{-1} Å^{-1}. The two dihedral angles, ϕ(H_1−C_1−O_1−H_1) and ω(O_6−C_6−C_5−H_5), were set to 0° and 60°, respectively. The initial model of the dextran 20mer with a dihedral angle of ψ(C_1−O_1−C_6−C_5) = 154° was build up using Polymer Builder in the Material Studio, and then the total charge of the molecule was also set to zero.

After one strand of the optimized structure of the **9merH** double helix was removed, the other **9merH** strand was arranged along the internal helical groove of the dextran 20mer strand. Finally, the energy minimization of the **9merH**−dextran 20mer heteroduplex was performed using the Smart Minimizer of the Discover module.

Acknowledgment. We thank Dr. Kawauchi (JST) for his help in the DOSY experiments.

Supporting Information Available: Details in the characterizations of the heteroduplexes formed from **9merH** and oligosaccharides. This material is available free of charge via the Internet at http://pubs.acs.org.

JA0730359

(21) Glasoe, P. K.; Long, F. A. *J. Phys. Chem.* **1960**, *64*, 188−190.